Journal of Institute of Science and Technology, 30(1), 139-147 (2025)
ISSN: 2467-9062 (print), e-ISSN: 2467-9240
https://doi.org/10.3126/jist.v30i1.78871

Research Article

SYNTHESIS, CHARACTERIZATION, ANTICANCER ACTIVITY, AND COMPUTATIONAL STUDY OF UMBELLIFERONE SCHIFF'S BASES

Anand Kumar Yadav[1,2], Siddhartha Das Pramanik[3], Partha Roy[3], Ranju Khatiwada[1], Achyut Adhikari[1], Paras Nath Yadav[1,]*
[1]Central Department of Chemistry, Institute of Science and Technology, Tribhuvan University, Kirtipur, Kathmandu, Nepal
[2]Department of Chemistry, Patan Multiple Campus, Patan Dhoka, Lalitpur, Nepal
[3]Department of Biosciences and Bioengineering, Indian Institute of Technology Roorkee, Uttarakhand-247667, India
**Correspondence: pnyadav219@gmail.com, paras.yadav@tu.edu.np*

(Received:** May 16, 2025; **Final Revision:** June 10, 2025; **Accepted:** June 12, 2025**)

ABSTRACT
4-Methylumbelliferone derivatives (1a–1c) were synthesized by condensing 3-acetyl-4-methylumbelliferone with hydroxyurea, urea, and thiourea. The synthesized new Schiff's bases were characterized by elemental analysis, ESI-HR MS, NMR, FT-IR, UV-Vis, and evaluated for their anticancer activity against the human prostate cancer (DU145) cell line. The tested compounds 1a, 1b, and 1c exhibited good anticancer efficacy in a dose-dependent manner in the tested cell line with IC_{50}; 122.78 μM, 109.65 μM, and 55.41μM, respectively in comparison to standard drug cisplatin. Furthermore, the ADMET profiling and Molecular Docking were carried with these synthesized compounds targeting protein Epidermal Growth Factor Receptor (EGFR) tyrosine Kinase (PDB ID 4HJO). Among these compounds, compound '1c' showed better intestinal absorption, positive Caco-2 permeability and negative AMES toxicity and hepatotoxicity. Also, it exhibited better interaction with the catalytically active site, Methionine at position 769 (MET 769) along with Glutamine (GLN 767), with binding energy, –10.3 kcal/mol.

Keywords: Anticancer activity, Molecular docking, Pharmacokinetics, Schiff's bases, Umbelliferone

INTRODUCTION
Cancer is a disease recognized by the uncontrolled cell division of the abnormal cells. In case of normal cells, the old cells die, and new normal cells are formed but when cancer develops in the body, old cells do not die but continue to grow to form abnormal cells. These abnormal cells are responsible for the inhibition of protein secretion of healthy cells and rapid replication of Deoxyribonucleic Acid (DNA) (Rawat & Vijaya Bhaskar Reddy, 2022). As cancer spreads, the cancerous cells lose their ability to respond to signals that control proliferation, cellular differentiation, survival, and death (Mahendran & Ponnuchamy, 2018). The metabolism of cancer cells is different from that of normal cells. Numerous metabolic processes that provide cellular building blocks and sustain the increased need for protein, lipid, and nucleic acid biosynthesis are upregulated in cancer cells (Lee et al., 2020). According to the International Agency for Research on Cancer (IARC), there are various cancer-causing agents like sedentary lifestyles, red meat, bacteria, alcohol, tobacco, Sunlight, not breastfeeding, obesity, viruses, fungi, and others (Blackadar, 2016). In Nepal, cancer is the third most common cause of death from non-communicable diseases, accounting for 9% of all annual casualties, with 20,508 new cases and 13,629 deaths from cancer, according to GLOBOCAN 2020 (Shilpakar et al., 2022). It is estimated that about 13% of all deaths is due to cancer worldwide (Al-Ishaq et al., 2020).

The ability of coumarins to establish noncovalent bonds with a variety of enzymes and receptors in living organisms accounts for their wide range of biological activities and uses (Pereira et al., 2018). A vast array of medicinal compounds, including antibacterial, antifungal, anticancer, antioxidant, antiviral, anti-inflammatory, anti-diabetic, anti-neurodegenerative, and anticoagulant agents, are now being developed from coumarin derivatives (Yadav et al., 2024). Coumarins have been found to reduce the risk of cancer and other cardiovascular diseases. Certain coumarins, such quercetin, esculetin, and umbelliferone, exhibit antioxidant qualities and prevent the cellular DNA from oxidative lesion (Garg et al., 2020). The synthesized 3-acetyl-4-hydroxycoumarin derivatives were evaluated *in vitro* for their anticancer potency against human breast cancer (MDA-MB-231 and MCF-7) cell lines by MTT assay. The new compounds showed strong anticancer efficacy against the tested MDA-MB-231 and MCF-7 cell lines with IC_{50} values 42.18–>100 μg/mL and 12.94–23.70 μg/mL, respectively (Shrestha et al., 2023).

Hydroxyurea is an anticancer drug, used in the treatment of cervical cancer, sickle-cell anaemia, and leukemia. The BrdU cell proliferation Enzyme-Linked Immunosorbent Assay (ELISA) was followed to investigate the antiproliferation effect of hydroxyurea against C6 (glioblastoma) and cervical cancer (HeLa) cells. The cytotoxicity % of hydroxyurea was found less than that of fluorouracil with IC_{50} values 77.45 μM and 69.33 μM against C6 and HeLa cells, respectively. At 250 μg/mL, it did not show any adverse effect on cell viability against tested cells (Karakus et al., 2020). Thiourea derivatives have been evaluated for their various biological activities including anticancer, antioxidant, antibacterial, antimalarial, anti-inflammatory, antituberculosis, and anti-Alzheimer (Agili, 2024). The conjugated urea drugs are being used in the therapy of different cancers such as

Linifanib for breast cancer, non- small cell lung carcinoma, colorectal cancer, and liver cancer, Sorafenib and Tivozanib for advanced renal cell carcinoma (Aroua et al., 2022). The umbelliferone (7-hydroxycoumarin) is a pharmacologically active compound. It is extensively distributed in plants like angelica, alexanders, asafoetica, cumin, celery, fennel, giant hogweed, parsley, and sanicle (Mazimba, 2017). The growing interest in synthesizing umbelliferone derivatives with pharmacological properties results from the compound's possible therapeutic benefits in treating different types of cancer, microbial infections, diabetes, inflammatory conditions, neurodegenerative diseases, and cardiovascular diseases (Kornicka et al., 2023). It reduces cell proliferation, induces apoptosis, and causes mitotic cell cycle arrest to significantly reduce the growth of ovarian cancer cells that are resistant to cisplatin (Wang & Wang, 2021).

In this study, urea, thiourea, and hydroxyurea derivatives of 4-methyl-7-hydroxycoumarin have been synthesized, characterized, and their anticancer activity is explored. The findings have established their anticancer potency.

EXPERIMENTAL

MATERIALS/METHODS

All chemicals utilized were of analytical reagent grade (AR). 4-Methylumbelliferone (97%), urea, thiourea, and hydroxyurea (Alfa Aesar), glacial acetic acid (99.7%) (Fischer Scientific), ethyl alcohol (99%) (Merck), human prostate cancer cell lines DU145 were procured from the National Centre for Cell Science (NCCS), Pune, India. All cell culture reagents were sourced from GIBCO (Invitrogen, USA). 3-(4,5-dimethylthiazol-2-yl)-2,5-diphenyl-2*H*-tetrazolium bromide (MTT), streptomycin, penicillin, cell culture-grade dimethyl sulfoxide (DMSO), Cisplatin, and other analytical-grade chemicals were obtained from HiMedia (Mumbai, India). UV-Vis spectra of the compounds were measured on Agilent Technologies Carry 60 UV-Vis spectrometer at the Central Department of Chemistry, Tribhuvan University (T.U.), Kathmandu, Nepal. The FTIR spectra were obtained using the Shimadzu IR tracer 100 instrument, in the range of 4000-400 cm^{-1} at Nepal Academy of Science and Technology (NAST), Lalitpur, Nepal. Data analysis for UV-Vis and FT-IR spectra was done using Origin Pro software, while IC_{50} (Half-maximal inhibitory concentration) values were determined using GraphPad Prism software. NMR spectra were recorded using a BRUKER BioSpin GmbH NMR spectrometer at the NMR Research Center, Indian Institute of Science, Bangalore, India. Elemental analysis (CHNS) by ELEMENTAR Vario EL III CHNS analyzer, and ESI-HRMS analysis using an LC-QTOF-HRMS spectrometer were obtained from Indian Institute of Technology, Madras, India. Melting points were determined on a PHILIPS HARIS melting point apparatus.

Synthesis of target compounds

Synthesis of compound (1a)

Acetylation of 7-hydroxycoumarin was carried out as mentioned in the protocol (Kumar et al., 2024) (Supporting data S1). 3-Acetyl-7-hydroxy-4-methylcoumarin (2.5 mmol, 0.54 g) was added to the solution of hydroxyurea (2.5 mmol, 0.19 g) in 15 mL of absolute ethanol (solvent). The mixture with catalytic amount of acetic acid (3 drops) was refluxed for 5 h at 78-80 °C. The reaction product was allowed to cool, precipitate was filtered, and dried at 40 °C overnight, and recrystallized from ethanol (Hamid & Salih, 2022). (**Scheme 1**).

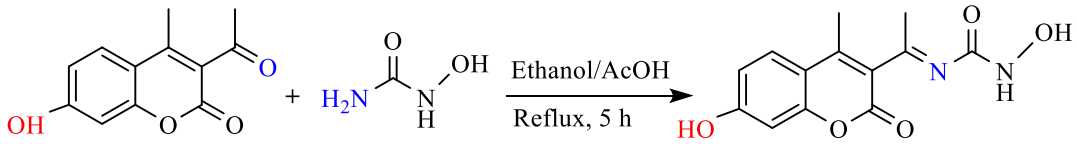

Scheme 1: Synthesis of compound 1a

Synthesis of compounds 1b and 1c

Urea 5 mmol (0.30 g)/ thiourea 5 mmol (0.38 g) was dissolved in 10 mL ethanol (solvent), and 10 mmol (2.18 g) of 3-acetyl-7-hydroxy-4-methylcoumarin was dissolved in 10 mL ethanol separately. These two solutions were mixed in a round-bottomed flask, 2 drops of acetic acid (catalyst) were added and refluxed for 4 h. Then the mixture was allowed to cool at room temperature and precipitate was filtered off, washed with cold ethanol, and dried in a desiccator overnight (Bahron et al., 2019) (**Scheme 2**).

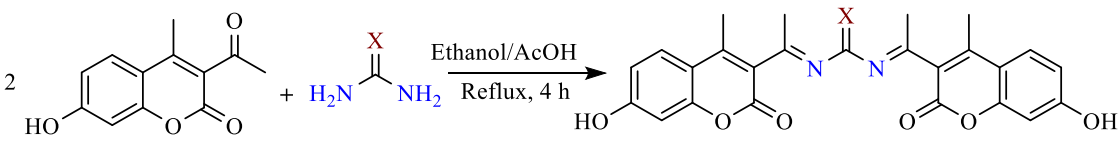

Scheme 2: Synthesis of compounds 1b (X=O), and 1c (X=S)

1a: (*E*)-1-hydroxy-3-(1-(7-hydroxy-4-methyl-2-oxo-2*H*-chromen-3-yl)ethylidene)urea

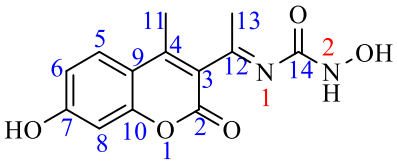

Figure 1: Structure and numbering of atoms in compound (1a)

Yield 47%, m. p. 193 °C, white powder, Elemental analysis: [$C_{13}H_{12}N_2O_5$] % found (calculated); C, 56.58 (56.52); H, 4.31 (4.25); N, 10.17 (10.13); ESI-HRMS, positive mode, $[M+H]^+$, found (calculated) m/z 277.0943 (277.0818) ; ^{1}H NMR (400 MHz, DMSO-d6), δ (ppm): 10.63 (s, 1H, C7-OH), 9.21 (s, 1H, N(2)-OH), 8.62 (s, 1H, N(2)-H), 7.83 (C5-H), 7.27 (C6-H), 7.18 (C8-H) (m, 3H Ar-H), 2.43 (s, 3H, CH_3, C11), 2.30 (s, 3H, CH_3, C13-H); ^{13}C NMR (400 MHz, DMSO-d6), δ (ppm): 168.80 (C=O, urea moiety), 159.39 (C=O, lactone), 154.82 (C=N, imine), 152.96 (C10), 152.88 (C7,7′), 147.10 (C4), 136.21 (C3), 126.40 (C5), 118.43 (C6), 113.71 (C9), 110.10 (C8), (Ar-C), 20.86 (CH_3-C11), 18.15 (CH_3-C13); IR, ν (selected bands, cm^{-1}): 3496 (b, O-H), 3401 (b, N-H, N2), 1762 (C=O, urea moiety), 1702 (C=O, lactone), 1620 (s, C=N), 1372 (N2-OH), 1198, 1016 (s, C-O-C, ester); UV-Vis (methanol, λmax nm): 280, sh (π-π*), 313, s (n- π*).

1b: 1,3-bis((*E*)-1-(7-hydroxy-4-methyl-2-oxo-2*H*-chromen-3-yl)ethylidene)urea

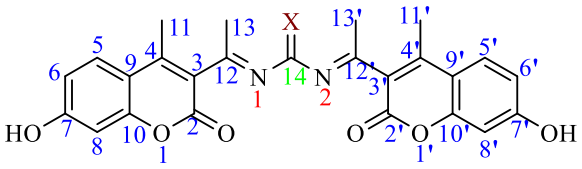

Figure 2: Structure and numbering of atoms in compound (1b, X= O; 1c, X= S)

Yield 54%, m. p. 207 °C, brownish powder, Elemental analysis: [$C_{25}H_{20}N_2O_7$] % found (calculated): C, 65.24 (65.21); H, 4.35 (4.30); N, 6.04 (6.01); ESI-HRMS, positive mode, found (calculated) $[M+H]^+$, m/z 461.3781 (461.1343) ; H^1 NMR (400 MHz, DMSO-d6), δ (ppm): 10.57 (s, 2H, C7, 7′-OH), 7.81 (C5, 5′-H), 7.26 (C6, 6′-H), 6.39 (C8, 8′-H), (m, 6H, Ar-H), 2.43 (s, 6H, CH_3, C11-C11′-H), 2.30 (6H, C13, C13′-H); C-13 NMR (400 MHz, DMSO-d6), δ (ppm): 168.79 (C=O, urea moiety), 159.61 (C=O, lactone), 153.50 (C=N, imine), 152.95 (C10,10′), 152.88 (C7,7′), 147.45 (C4,4′), 130.93 (C3,3′), 126.40 (C5,5′), 118.42 (C6,6′), 113.71 (C9,9′), 110.10 (C8,8′), (Ar-C), 20.85 (CH_3- C11), 18.14 (CH_3-C13); IR, ν (selected bands, cm^{-1}): 3159 (b, O-H), 3049 (CH, Ar), 1765 (C=O, urea moiety), 1699 (C=O, lactone),1608 (s, C=N), 1192, 1014 (s, C-O, ester); UV-Vis (methanol, λmax nm): 280 sh (π-π*), 312 sh (n- π*).

1c: 1,3-bis((*E*)-1-(7-hydroxy-4-methyl-2-oxo-2*H*-chromen-3-yl)ethylidene)thiourea

Yield 51%, m. p. 206 °C, powder, Elemental analysis: [$C_{25}H_{20}N_2O_6S$] % found (calculated); C, 63..06 (63.02); H, 4.27 (4.23); N, 5.86 (5.81); S, 7.70 (6.59); ESI-HRMS, positive mode, found (calculated) $[M+H]^+$, m/z 477.1525 (477.1114); H^1 NMR (400 MHz, DMSO-d6), δ (ppm): 10.53 (s, 2H, C7,7′- OH), 7.81 (C5, 5′-H), 7.26 (C6, 6′-H), 6.39 (C8, 8′-H), (m, 6H Ar-H), 2.43 (s, 6H, CH_3-C11, C11′-H), 2.30 (s, 6H, C13, C13′-H); C-13 NMR (400 MHz, DMSO-d6), δ (ppm): 180.12 (C=S), 159.60 (C=O, lactone), 153.50 (C=N, imine), 152.94 (C10, 10′-H), 152.87 (C7, 7′-H), 147.07 (C4, 4′-H), 136.59 (C3, 3′-H), 126.40 (C5, 5′-H), 118.42 (C6, 6′-H), 113.71 (C9, 9′-H), 110.09 (C8, 8′-H), (Ar-C), 20.85 (CH_3-C11), 18.14 (CH_3-C13), IR, ν (selected bands, cm^{-1}): 3404 (b, O-H), 3051 (CH, Ar), 1698 (C=O, lactone), 1616 (s, C=N), 1266 (C=S, thiourea moiety), 1193, 1015 (s, C-O, ester); UV-Vis (methanol, λmax nm): 279 sh (π-π*), 312 sh (n- π*).

Biological study

Cell Culture

Prostate cancer (DU145) cells were cultured and grown in RPMI1640 medium (Himedia, Mumbai, India) supplemented with 10% (v/v) fetal bovine serum (GIBCO, Invitrogen, USA) and 1% antibiotics (100 mg/mL streptomycin and U/mL of penicillin) (Himedia, Mumbai, India). Cells were maintained in a humidified incubator at 5% CO_2 and 37 °C.

Cell viability assay

The MTT assay was performed according to the protocol described previously (Baul et al., 2024). Briefly, 5 × 10^3 cells were seeded in a 96-well plate. After 24 hours of incubation, the culture media was replaced with fresh media containing different concentrations of test compounds (10, 50 and 100 µM). The cells were then incubated for 24 hours in a humidified incubator at 5%

CO_2 and 37 °C. At the end of the incubation, 20 µL of MTT reagent (5 mg/mL) was added and allowed to incubate for another 4 hours. Then, 150 µL of DMSO was added to solubilize the formazan crystals in each well. Absorbance was measured at 570 nm using a multimode plate reader (Fluostar Omega, BMG LabTech, Germany). Cell viability percentage was calculated using the following equation: Cell viability (%) = (Absorbance of cells exposed to the sample/Absorbance of untreated cells) × 100.

Computational Study

Molecular Docking Studies

Receptor and Ligand Preparation

The crystal structure of the target protein was obtained from the Protein Data Bank (https://www.rcsb.org/) and processed using BIOVIA Discovery Studio Visualizer 2020. Before the preparation, the properties of any co-crystallized ligands were recorded. All water molecules, ligands, and other heteroatoms were removed, and polar hydrogen atoms, along with Kollman charges, were added to the protein structure. The compounds which are synthesized their structures were drawn on ChemDraw and converted into mol file then the file was converted into the .pdb format in Discovery Studio and were optimized for docking and were saved in .pdbqt format using AutoDock Vina. There are many other computation softwares for molecular docking, such as molecular operating environment (MOE), genetic optimization for ligand docking (GOLD), GLIDE, HADDOCK, PyRx, etc. AutoDock Vina is a powerful open source docking tool within AutoDock suite which is widely recognized and utilized. It is effective for docking drug-like compounds to protein (Eberhardt et al., 2021).

Pharmacokinetics analysis

The pharmacokinetics analysis provides insight into the potential efficacy of the drug candidates and indicates that the synthesized compounds may possess properties consistent with orally administered drugs. The canonical SMILES (Simplified Molecular Input Line Entry System) representation of the compounds was submitted to the pkCSM web servers for pharmacokinetic predictions.

RESULTS AND DISCUSSION

ESI-HRMS

HRMS ESI positive mode mass spectrometry helps to recognize the molecular ion with great resolution and precision. The soft ionization method yields protonated molecular ions with less or no fragmentation and produces a single peak (Lin et al., 2024). The ideal conditions ensure that the peak precisely matches the mass of the protonated molecular ion, improving spectrum purity and yielding accurate and reliable molecular mass data. The protonated molecular ion $[M + H]^+$ peaks for the new compounds 1a, 1b, and 1c; m/z: found (calculated); 277.0943 (277.0818), 461.3781 (461.1343), and 477.1525 (477.1114), respectively, were obtained (Shrestha et al., 2024). The proposed structures of the synthesized compounds are consistent with the mass spectral data, (Supporting data S2-S4).

NMR spectroscopy

In the ^{1}H NMR spectra of compounds 1a, 1b, and 1c, the singlet signals at 10.63, 10.57, and 10.53 ppm, respectively, were attributed to OH group (Toan & Thanh, 2021). The downfield signals of OH group may be due to conjugated benzopyran ring and intermolecular hydrogen bonding. The spectrum of compound '1a' showed two singlet signal at 9.21 ppm, and 8.62 ppm, can be attributed to N2-OH and N2-H, respectively (Karakus et al., 2020). The aromatic protons in coumarin (C5-H, C6-H, and C8-H) in the spectra of compounds 1a, 1b, and 1c appeared as multiplet signals at 7.83–7.81 ppm (C5-H), 7.27–7.20 ppm (C6-H), and 7.18–6.39 ppm (C8-H), respectively (Manojkumar et al., 2009). The aromatic protons' signals at 7.83–6.39 ppm downfield is because of electron-withdrawing effect of pyrone lactone group. The singlet of CH_3 proton of coumarin (C11-H, C11'-H) appeared towards the up-field position at 2.43 ppm, also, the singlet of proton of CH_3, linked to azomethine (C13-H, C13'-H) appeared at 2.30 ppm (Dawood et al., 2015). (Supporting data S5-S7).

The ^{13}C NMR spectra of the compound '1c' exhibited resonance due to highly polar thiocarbonyl carbons (C=S), towards downfield region at 180.12 ppm (Thanh et al., 2015). In the spectra of compounds 1a, and 1b, the chemical shift which located at range of 168.80–168.79 ppm is assigned to carbonyl (C=O, urea moiety) group. The two distinct peaks of more polar aromatic carbon atoms (C10 and C7) of coumarin moiety were observed at 152.96–152.94 ppm and 152.88-152.87 ppm, respectively, other aromatic carbon atoms of coumarin were observed at 126.40–110.09 ppm (Yang et al., 2014). The carbon atoms C4, and C3 of pyran ring of these compounds exhibited resonance signals at 147.45–147.10 ppm, and 136.59–130.93 ppm, respectively (Rahman et al., 2017), the carbons in the heterocyclic ring undergo a chemical shift that is positioned downfield because of the oxygen atom in the pyrone ring (Arjunan et al., 2013). The ^{13}C NMR spectra of the compounds 1a, 1b, and 1c showed the appearance of signals in the region of 159.61–159.39 ppm, is belonging to the (C=O, lactone), and signal at 154.82–153.50 ppm was assigned to imine (C=N) groups, (Aroua et al., 2022). The methyl carbons' (C11) peaks for these compounds were observed at 20.86–20.85 ppm whereas the methyl carbons (C13) of the compounds exhibited resonance signals at 18.15–18.14 ppm (Jevtić et al., 2013), (Supporting data S8-S10).

FT-IR spectroscopy

The FTIR spectra the compounds 1a, 1b, and 1c were found quite similar in terms of absorption peaks. The absorption peak of the υ(O-H, Phenolic) group observed as broad peak at the range of 3496–3159 cm^{-1}, whereas the spectra of the compound '1a' exhibited broad band at 3401 cm^{-1}, and 1372 cm^{-1} which was attributed to υ(N2H), and υ(N2-OH) groups, respectively (Tantaru et

al., 2017). The weak absorption peaks were observed in the spectra at 3051–3049 cm^{-1} that was assigned to the stretching vibration υ(Ar, C-H). The parent compound 3-acetyl-7-hydroxycoumarin's IR spectra exhibits a strong band at 1718 cm^{-1} due to the carbonyl (C=O, lactone) stretching frequency and a band at 1683 cm^{-1} attributed to the acetyl group's (C=O) stretching frequency. The new stretching frequency at 1620, 1608, and 1616 cm^{-1} were observed on condensing with hydroxyurea, urea, and thiourea, for the compounds 1a, 1b, and 1c, respectively, that confirms the formation of the imine (C=N) bond (Ranade et al., 2016). The band appeared at 1266 cm^{-1}, was assigned to υ(C=S), thiourea moiety, for the compounds '1c' (Alwan, 2018). The C-O stretching and bending vibrations are caused by the oxygen in the pyrone ring. The υ(C-O) stretching band was identified at 1198-1192 cm^{-1} and 1016-1014 cm^{-1} (Vekariya et al., 2017), (Supporting data S11-S13).

UV-Vis spectroscopy

The UV-Vis spectra of the synthesized compounds (1a-1c) were studied at a concentration of 1×10^{-5} M in methanol in the range of 200–600 nm at room temperature. The spectra of the compounds exhibited two prominent absorption peaks. The first peak found at 279–280 nm, was assigned to the π→π* transitions of the coumarin ring and n→π* transisition from C=O or C=S group. The second peak observed at 313–312 nm is because of n→π*, transitions of imine (C=N) group and minor contribution from thionyl group (C=S) in thiourea derivative. A bathochromic shift was observed due to extended conjugation on formation of Schiff's bases (Verma et al., 2019). The lone pair electrons at nitrogen of azomethine group is excited to the π* orbital of the double bond and as it is conjugated with aromatic ring of coumarin, the absorption band shifts to longer wavelength in UV-Vis spectrum. The weaker electronic interaction of the C=N bond is responsible for the absorption shoulder peak (Ketata et al., 2012), (Supporting data S14-S16).

***In vitro* cell viability test (MTT assay)**

Anticancer potential of compounds in Human prostate cancer (DU145) cell line

Here, we used the human prostate cancer cell line (DU145) to study the cell cytotoxicity of test compounds. The test compounds (1a, 1b and 1c) were dissolved in DMSO (vehicle) and the control cell samples without DMSO taken were used as controls. Both the cells were grown for 24 h before the treatment of the complexes. Furthermore, as mentioned in the methodology section, both the cells were treated with 10 µM, 50 µM, and 100 µM of test compounds. The effect of test compounds was evaluated after exposure for 24 h. For comparing the cytotoxicity, we also used a standard drug Cisplatin, against the DU145 cell line as a positive control. The results were calculated as a percentage of cells killed with respect to the concentrations of test compounds (10, 50 and 100 µM) as shown in Fig. 3. The 3-(4,5-dimethylthiazol-2-yl)-2,5-diphenyl-2*H*-tetrazolium bromide (MTT) assay revealed that the 1c showed remarkable activity against the cancer cell line DU145 compared to 1a and 1b. The IC_{50} of the test compounds 1a, 1b, and 1c was found to be 122.78 µM, 109.65 µM, and 55.41µM, respectively. In contrast, CDDP eradicated approximately 50% of cells at a concentration of 30 µM. The potent compound '**1c**' killed up to 21.07%, 53.58%, and 71.89% tumour cells at 10, 50, and 100 µM concentrations, respectively. The standard drug cisplatin killed up to 50.23% of the cells at a 30 µM concentration. The cell viability tests showed that '1c' has the potential to stop the growth of cancer cells in a concentration-dependent manner.

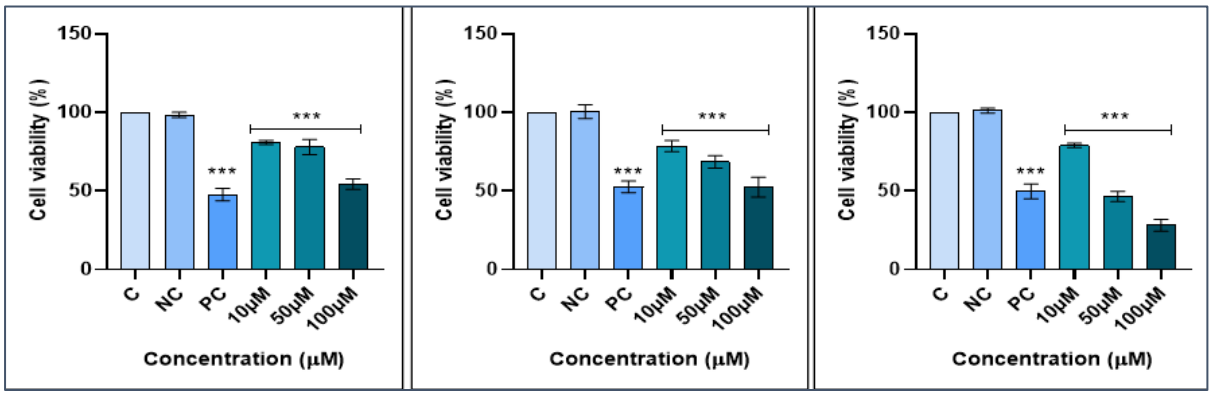

(1a) (1b) (1c)

Figure 3: Cytotoxic effects of 1a, 1b, and 1c against DU145 prostate cancer cells after 24 h treatment. ***, **, and *, signify $p < 0.001$, $p < 0.01$, and $p < 0.05$, respectively. Group C indicates control, NC indicates negative control, and PC indicates positive control.

Hydrogen bonding interactions were observed between the active site residue MET 769 (Park et al., 2012) of the target protein 4HJO and all three compounds: 1a, 1b, and 1c. Among them, compound '1b' demonstrated the strongest binding affinity, exhibiting the lowest binding energy of -11.5 Kcal/mol, followed by compound '1c' at -10.3 Kcal/mol, and compound '1a' at -8.2 Kcal/mol. Compound '1a' also displayed additional non-covalent interactions, including Pi-Sigma and Pi-Alkyl interactions with residues such as LEU820, ALA 719, LEU 694, and VAL 702. Compound '1b' showed a more diverse interaction profile, forming Pi-Sigma, Pi-Cation,

Pi-Anion, Pi-Alkyl, and Pi-Pi T-shaped interactions with amino acids LEU 694, VAL 702, LYS 721, ARG 817, PHE 699, ASP 813, and PRO 853. Notably, compound '**1c**' formed an additional hydrogen bond with a second key active site residue, GLN 767, and also engaged in various stabilizing interactions such as Pi-Sigma, Pi-Alkyl, Carbon-Hydrogen bonding, and Pi-Donor Hydrogen bonding distance to MET 769, measured at 3.03Å, suggesting a more favorable and stable complex formation. After analyzing the pharmacokinetic profiles, binding energies, and detailed interaction, compound '**1c**' stands out as the most promising candidate for further optimization and development.

Molecular docking

Table 1: Molecular Docking results

Compounds	Binding Affinity (kcal/mol)	Amino acid Residues	Interaction Type	Interaction Distance Å
1a	-8.2	MET 769, ALA 719, LEU 694, LEU 820, VAL 702	Hydrogen bond, Pi-Sigma bond, Pi-Alkyl bond	3.40, 4.82, 5.03,3.72, 3.84, 5.12, 4.46, 7.01, 4.56
1b	-11.5	MET 769, LEU 694, VAL 702, LYS 721, ARG 817, PHE 699, ASP 813, PRO 853	Hydrogen bond, Pi-Sigma, Pi-Cation, Pi-Anion, Pi-Sigma, Pi-Alkyl, Pi-Pi T-Shaped	3.18, 5.00, 5.03, 5.09, 3.40, 4.57, 4.21, 4.90, 4.94, 3.45
1c	-10.3	MET 769, GLN 767, ALA 719, LEU 694, LEU 768, ALA 820, VAL 702, ALA 698, LYS 851	Hydrogen bond, Carbon-Hydrogen Bond, Pi-Donor Hydrogen Bond, Pi-Sigma, Pi-Alkyl	3.03, 3.13, 4.36,3.20, 3.90,3.72, 5.46, 3.97, 3.19, 4.07, 3.19

When conducting molecular docking studies, it's common practice to consider compounds with a binding affinity of less than -7.0 kcal/mol as potent (Terefe & Ghosh, 2022). Additionally, a thorough analysis of docking results involves examining the specific residues that interact with the ligand and types of interaction formed. In this manuscript, the compounds showed lower binding affinity than -7.0 kcal/mol and the ligand interacted with active amino acid residues through H-bonds. These findings are suitable to predict the synthesized compounds showing anticancer property. The 2D-structure of all three compounds is shown below (Fig. 4).

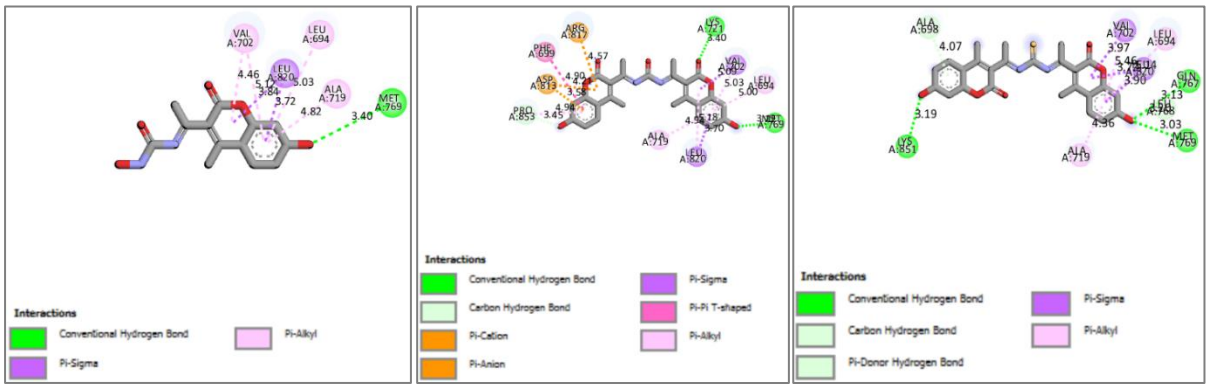

(1a) (1b) (1c)

Figure 4: 2D structures of complexes of compounds (1a, 1b, and 1c) with EGFR

Pharmacokinetics analysis

The synthesized compounds 1a, 1b, and 1c were subjected to pharmacokinetic ADMET analysis using the pkCSM web server. The analysis evaluated several parameters including human intestinal absorption (HIA), Caco-2 cell permeability, volume of distribution (logVDss), blood-brain barrier (BBB) permeability, central nervous system (CNS) permeability, metabolism (CYP450 enzyme inhibition), total clearance (excretion), as well as AMES toxicity and hepatotoxicity (Muehlbacher et al., 2011). The pharmacokinetic properties of these Schiff's bases are systematically tabulated (**Table 2**).

Table 2: Pharmacokinetic analysis of the compounds

Parameters ↓	Compounds →	1a	1b	1c
Absorption	Water solubility (log mol/L)	-3.073	- 4.558	- 4.452
	CaCO2 Permeability (log Papp 10-6 cm/s)	-0.027	- 0.009	0.582
	Intestinal absorption (% absorbed)	79.919	90.001	91.207
	Skin permeability (log Kp)	-3.305	-2.783	-2.790
Distribution	VDss (Human, log L/Kg)	-0.820	-0.294	-0.221
	BBB permeability (log BB)	-1.117	-1.042	-0.976
	CNS permeability (log PS)	-3.348	-1.85	-1.822
Metabolism	CYP1A2	Yes	No	No
	CYP2C19	No	Yes	Yes
	CYP2C9	No	Yes	Yes
	CYP2D6	No	No	No
	CYP3A4	No	Yes	Yes
Excretion	Total clearance	0.753	0.831	-0.248
	Renal OCT2 substrate Clearance	No	No	No
Toxicity	Ames Toxicity	Yes	No	No
	Hepatotoxicity	No	No	No
	Rat Oral Toxicity (LD_{50})	2.954	2.625	2.515

All three compounds demonstrated high intestinal absorption (>70%). Among them, compound '1c' exhibited the most favorable profile, with enhanced absorption and positive Caco-2 permeability, and showed no AMES toxicity or hepatotoxicity. However, it was found to inhibit CYP2C19, CYP2C9, and CYP3A4 enzymes (Lagorce et al., 2017). Similarly, compound '1b' also tested negative for AMES toxicity and hepatotoxicity, showed moderate water solubility, and inhibited several CYP enzymes. In contrast, compound '1a' was positive for AMES toxicity, indicating potential mutagenicity, and inhibited CYP1A2, which may lead to drug-drug interactions. Based on the overall ADMET profile, compound '1c' appears to have the most promising pharmacokinetic properties for further development.

CONCLUSIONS

The synthesized Schiff's bases exhibited good anticancer potency against DU145 (human prostate cancer) cell line with IC_{50} 55.41–122.78 µM. The compound 1,3-bis((*E*)-1-(7-hydroxy-4-methyl-2-oxo-2*H*-chromen-3-yl)ethylidene)thiourea (1c) was found the most active against the tested cell line, it is supported by *in silico* study also. Structure-activity relationship (SAR) study signifies in compound '1c' Sulphur is more polarisable, C=S increases lipophilicity, and facilitate membrane permeability. Moreover, the results are further confirmed by the Pharmacokinetics and Molecular Docking where compound '1c' showed the outstanding results on orally administered properties and binding interaction and binding energies against the EGFR tyrosine Kinase (PDB ID 4HJO). This study shows compound '1c' could be a potential candidate for anticancer efficacy with certain modification in its structure.

ACKNOWLEDGEMENTS

We sincerely acknowledge Nepal Academy of Science and Technology, Lalitpur, Nepal for UV and FT-IR data, Department of Biosciences and Bioengineering, Indian Institute of Technology Roorkee, Roorkee, Uttarakhand, India for anticancer screening. Indian Institute of Technology (IIT) Madras, India, for the CHNS, and HR-MS ESI data, Indian Institute of Science (IISc), Bangalore, India, for NMR data.

AUTHOR CONTRIBUTIONS

Anand Kumar Yadav: Writing original draft, Methodology, Synthesis and Characterization of Compounds; Partha Roy: Anticancer screening supervision; Siddhartha Das Pramanik: Anticancer screening and drafting; Ranju Khatiwada: Software; Achyut Adhikari: Conceptualization; Paras Nath Yadav: Supervision.

CONFLICTS OF INTEREST

The authors declare no conflict of interest.

DATA AVAILABILITY

The data that is used to create figures and tables are available upon request to the corresponding author.

REFERENCES

Agili, F.A. (2024). Biological applications of thiourea derivatives: detailed review. *Chemistry (Switzerland)*, *6*(3), 435–468. https://doi.org/10.3390/chemistry6030025.

Al-Ishaq, R.K., Overy, A.J., & Büsselberg, D. (2020). Phytochemicals and gastrointestinal cancer: Cellular mechanisms and effects to change cancer progression. *Biomolecules*, *10*(1), 105. https://doi.org/10.3390/biom10010105.

Alwan, W.M. (2018). Synthesis, characterization and the corrosion inhibition study of two Schiff base ligands derived from urea and thiourea and their complexes with Cu(II) and Hg(II) ions. *Journal of Physics: Conference Series*, *1003*(1), 012017. https://doi.org/10.1088/17426596/1003/1/012017.

Arjunan, V., Sakiladevi, S., Marchewka, M.K., & Mohan, S. (2013). FTIR, FT-Raman, FT-NMR and quantum chemical investigations of 3-acetylcoumarin. *Spectrochimica Acta - Part A: Molecular and Biomolecular Spectroscopy*, *109*, 79–89. https://doi.org/10.1016/j.saa.2013.01.100.

Aroua, L.M., Al-Hakimi, A.N., Abdulghani, M.A.M., & Alhag, S.K. (2022). Cytotoxic urea Schiff base complexes for multidrug discovery as anticancer activity and low in vivo oral assessing toxicity. *Arabian Journal of Chemistry*, *15*(8), 103986. https://doi.org/10.1016/j.arabjc.2022.103986.

Bahron, H., Khaidir, S.S., Tajuddin, A.M., Ramasamy, K., & Yamin, B.M. (2019). Synthesis, characterization and anticancer activity of mono- and dinuclear Ni(II) and Co(II) complexes of a Schiff base derived from o-vanillin. *Polyhedron*, *161*(Ii), 84–92. https://doi.org/10.1016/j.poly.2018.12.055.

Blackadar, C.B. (2016). Historical review of the causes of cancer. *World Journal of Clinical Oncology*, *7*(1), 54–86. https://doi.org/10.5306/wjco.v7.i1.54.

Dawood, D.H., Batran, R.Z., Farghaly, T.A., Khedr, M.A., & Abdulla, M.M. (2015). New coumarin derivatives as potent selective COX-2 inhibitors: synthesis, anti-inflammatory, QSAR, and molecular modeling studies. *Archiv Der Pharmazie*, *348*(12), 875–888. https://doi.org/10.1002/ardp.201500274.

Eberhardt, J., Santos-Martins, D., Tillack, A.F., & Forli, S. (2021). AutoDock Vina 1.2.0: New docking methods, expanded force field, and Python bindings. *Journal of Chemical Information and Modeling*, *61*(8), 3891–3898. https://doi.org/10.1021/acs.jcim.1c00203.

Garg, S.S., Gupta, J., Sharma, S., & Sahu, D. (2020). An insight into the therapeutic applications of coumarin compounds and their mechanisms of action. *European Journal of Pharmaceutical Sciences*, *152*, 105424. https://doi.org/10.1016/j.ejps.2020.105424.

Hamid, S.J., & Salih, T. (2022). Design, synthesis, and anti-inflammatory activity of some coumarin Schiff base derivatives: In silico and in vitro study. *Drug Design, Development and Therapy*, *16*, 2275–2288. https://doi.org/10.2147/DDDT.S364746.

Jevtić, V.V., Pešić, M., Radić, G.P., Vuković, N., Sukdolak, S., Klisurić, O., Podolski-Renić, A., Tanić, N., & Trifunović, S.R. (2013). Synthesis, characterization and cytotoxicity of a new palladium(II) complex with a coumarin-derived ligand. Crystal structure of 4-hydroxy-3-(1-(p-tolylimino)ethyl)-2H-chromen-2-one-palladium(II) complex. *Journal of Molecular Structure*, *1040*, 216–220. https://doi.org/10.1016/j.molstruc.2013.03.013.

Karakus, G., Kaplan Can, H., & Sahin Yaglioglu, A. (2020). Synthesis, structural characterization, thermal behavior and cytotoxic/antiproliferative activity assessments of poly(maleic anhydride-alt-acrylic acid)/hydroxyurea polymer/drug conjugate. *Journal of Molecular Structure*, *1210*, 127989. https://doi.org/10.1016/j.molstruc.2020.127989.

Ketata, I., Mechi, L., Ayed, T. Ben, Dusek, M., Petricek, V., & Hassen, R. (2012). Synthesis, characterization, spectroscopic and crystallographic investigation of Cobalt(III) schiff base complex with two perpendicular diamine coumarin ligands. *Open Journal of Inorganic Chemistry*, *2*(02), 33–39. https://doi.org/10.4236/ojic.2012.22006.

Kornicka, A., Balewski, Ł., Lahutta, M., & Kokoszka, J. (2023). Umbelliferone and its synthetic derivatives as suitable molecules for the development of agents with biological activities: a review of their pharmacological and therapeutic potential. *Pharmaceuticals*, *16*(12), 1732. https://doi.org/10.3390/ph16121732.

Kumar, A., Singh, N., Silwal, M., Adhikari, A., & Nath, P. (2024). Synthesis , characterization , anticancer activity , molecular docking and DFT calculation of 3-acetylcoumarin thiosemicarbazones and Schiff ' s bases. *Results in Chemistry*, *11*, 101794. https://doi.org/10.1016/j.rechem.2024.101794.

Lagorce, D., Douguet, D., Miteva, M.A., & Villoutreix, B.O. (2017). Computational analysis of calculated physicochemical and ADMET properties of protein-protein interaction inhibitors. *Scientific Reports*, *7*, 1–15. https://doi.org/10.1038/srep46277.

Lee, N., Spears, M.E., Carlisle, A.E., & Kim, D. (2020). Endogenous toxic metabolites and implications in cancer therapy. *Oncogene*, *39*(35), 5709–5720. https://doi.org/10.1038/s41388-020-01395-9.

Lin, L., Sun, S., & Yu, Q. (2024). Explore the feasibility of electrospray ionization high-resolution mass spectrometry in elemental analysis. *Spectrochimica Acta - Part B Atomic Spectroscopy*, *217*, 106959. https://doi.org/10.1016/j.sab.2024.106959.

Mahendran, G., & Ponnuchamy, K. (2018). Coumarin-gold nanoparticle bioconjugates: Preparation, antioxidant, and cytotoxic effects against MCF-7 breast cancer cells. *Applied Nanoscience (Switzerland)*, *8*(3), 447–453. https://doi.org/10.1007/s13204-018-0816-7.

Manojkumar, P., Ravi, T., & Subbuchettiar, G. (2009). Synthesis of coumarin heterocyclic derivatives with antioxidant activity and *in vitro* cytotoxic activity against tumour cells. *Acta Pharmaceutica*, *59*(2), 159–170. https://doi.org/10.2478/v10007-009-0018-7.

Mazimba, O. (2017). Umbelliferone: Sources, chemistry and bioactivities review. *Bulletin of Faculty of Pharmacy, Cairo University*, *55*(2), 223–232. https://doi.org/10.1016/j.bfopcu.2017.05.001.

Muehlbacher, M., Spitzer, G.M., Liedl, K.R., & Kornhuber, J. (2011). Qualitative prediction of blood-brain barrier permeability on a large and refined dataset. *Journal of Computer-Aided Molecular Design*, *25*(12), 1095–1106. https://doi.org/10.1007/s10822-011-9478-1.

Park, J.H., Liu, Y., Lemmon, M.A., & Radhakrishnan, R. (2012). Erlotinib binds both inactive and active conformations of the EGFR tyrosine kinase domain. *Biochemical Journal*, *448*(3), 417–423.

https://doi.org/10.1042/BJ20121513.

Pereira, T. M., Franco, D. P., Vitorio, F., & Kummerle, A. E. (2018). Coumarin compounds in medicinal chemistry: Some important examples from the last years. *Current Topics in Medicinal Chemistry*, *18*(2), 124–148. https://doi.org/10.2174/1568026618666180329115523.

Rahman, K.N.A., Haribabu, J., Balachandran, C., Bhuvanesh, N.S.P., Karvembu, R., & Sreekanth, A. (2017). Copper, nickel and zinc complexes of 3-acetyl coumarin thiosemicarbazone: Synthesis, characterization and in vitro evaluation of cytotoxicity and DNA/protein binding properties. *Polyhedron*, *135*, 26–35. https://doi.org/10.1016/j.poly.2017.06.044.

Ranade, D.S., Bapat, A.M., Ramteke, S.N., Joshi, B.N., Roussel, P., Tomas, A., Deschamps, P., & Kulkarni, P.P. (2016). Thiosemicarbazone modification of 3-acetyl coumarin inhibits Aβ peptide aggregation and protect against Aβ-induced cytotoxicity. *European Journal of Medicinal Chemistry*, *121*, 803–809. https://doi.org/10.1016/j.ejmech.2015.07.028.

Rawat, A., & Vijaya Bhaskar Reddy, A. (2022). Recent advances on anticancer activity of coumarin derivatives. *European Journal of Medicinal Chemistry Reports*, *5*, 100038. https://doi.org/10.1016/j.ejmcr.2022.100038.

Shilpakar, R., Paudel, B.D., Sharma, R., Silwal, S.R., Sapkota, R., Shrestha, P., Dulal, S., Piya, M.K., Tuladhar, S.M., Neupane, P., Dhimal, M., Niroula, A., & Uprety, D. (2022). Lung cancer in Nepal. *Journal of Thoracic Oncology*, *17*(1), 22–29. https://doi.org/10.1016/j.jtho.2021.10.020.

Shrestha, R.M., Mahiya, K., Shrestha, A., Mohanty, S.R., Yadav, S.K., & Yadav, P.N. (2024). Synthesis, characterization, and anticancer potency of coumarin-derived thiosemicarbazones and their Copper(II) complexes. *Inorganic Chemistry Communications*, *161*, 112142. https://doi.org/10.1016/j.inoche.2024.112142.

Tantaru, G., Poiata, A., Bibire, N., Panainte, A.D., Apostu, M., & Vieriu, M. (2017). Synthesis and biological evaluation of a new Schiff base and its Cu(II) complex. *Revista de Chimie*, *68*(3), 586–588. https://doi.org/10.37358/rc.17.3.5506.

Terefe, E.M., & Ghosh, A. (2022). Molecular docking, validation, dynamics simulations, and pharmacokinetic prediction of phytochemicals isolated from *Croton dichogamus* against the HIV-1 reverse transcriptase. *Bioinformatics and Biology Insights*, *16*, 11779322221125604. https://doi.org/10.1177/11779322221125605.

Thanh, N.D., Van, H.T.K., & Thu, T.T. (2015). Synthesis and characterization of some novel thiosemicarbazones of substituted benzaldehydes and N-(Hepta-O-Acetyl-β-D-Lactosyl) thiosemicarbazide. *Journal of Carbohydrate Chemistry*, *34*, 514–544. https://doi.org/10.1080/07328303.2015.1114119.

Toan, V.N., & Thanh, N.D. (2021). Synthesis and antiproliferative activity of hybrid thiosemicarbazone derivatives bearing coumarin and d-galactose moieties with EGFR inhibitory activity and molecular docking study. *Medicinal Chemistry Research*, *30*(10), 1868–1885. https://doi.org/10.1007/s00044-021-02773-y.

Vekariya, R.H., Patel, K.D., Rajani, D.P., Rajani, S.D., & Patel, H.D. (2017). A one pot, three component synthesis of coumarin hybrid thiosemicarbazone derivatives and their antimicrobial evolution. *Journal of the Association of Arab Universities for Basic and Applied Sciences*, *23*, 10–19. https://doi.org/10.1016/j.jaubas.2016.04.002.

Verma, S.K., Savani, C., & Singh, V.K. (2019). Synthesis, photophysical, thermal and crystallographic studies of 3-Aminocoumarin based monobasic κ3-O,N,O-tridentate/ κ2-N,O-bidentate Schiff base divalent complexes. *Chemistry Select*, *4*(48), 14244–14252. https://doi.org/10.1002/slct.201903988.

Wang, H., & Wang, Y. (2021). Anticancer effect of 7-hydroxycoumarin in cisplatin-resistant ovarian cancer cell is mediated via apoptosis induction, caspase activation and cell cycle arrest at G2M phase. *Tropical Journal of Pharmaceutical Research*, *20*(2), 281–286. https://doi.org/10.4314/tjpr.v20i2.9.

Yadav, A.K., Maharjan Shrestha, R., & Yadav, P.N. (2024). Anticancer mechanism of coumarin-based derivatives. *European Journal of Medicinal Chemistry*, *267*, 116179. https://doi.org/10.1016/j.ejmech.2024.116179.

Yang, Y., Liu, Q.W., Shi, Y., Song, Z.G., Jin, Y.H., & Liu, Z.Q. (2014). Design and synthesis of coumarin-3-acylamino derivatives to scavenge radicals and to protect DNA. *European Journal of Medicinal Chemistry*, *84*, 1–7. https://doi.org/10.1016/j.ejmech.2014.07.009.